Chemical Engineering Journal 168 (2011) 1346–1351

Contents lists available at ScienceDirect

Chemical Engineering Journal

journal homepage: www.elsevier.com/locate/cej

Surface-modified cerium oxide nanoparticles synthesized continuously in supercritical methanol: Study of dispersion stability in ethylene glycol medium

Bambang Veriansyah [a], Myung-Suk Chun [b,*], Jaehoon Kim [a,**]

[a] Supercritical Fluid Research Laboratory, Clean Energy Center, Energy Division, Korea Institute of Science and Technology (KIST), 39-1 Hawolgok-dong, Seongbuk-gu, Seoul, 136-791, Republic of Korea
[b] Complex Fluids Laboratory, Korea Institute of Science and Technology (KIST), 39-1 Hawolgok-dong, Seongbuk-gu, Seoul, 136-791, Republic of Korea

ARTICLE INFO

Article history:
Received 22 June 2010
Received in revised form 9 December 2010
Accepted 16 December 2010

Keywords:
Nanoparticle
Dispersion stability
DLVO interaction
Electrostatic repulsion
van der Waals attraction
Hydrophobic/hydrophilic interaction

ABSTRACT

Dispersion stability of surface-modified cerium oxide (CeO_2) nanoparticles in ethylene glycol is examined and the experimental stability results are compared with an extended DLVO model consisting of electrostatic, van der Waals, and hydrophobic/hydrophilic interactions. Unmodified, decanoic acid-modified and oleic acid-modified CeO_2 nanoparticles are synthesized continuously in supercritical methanol (scMeOH). The surface charge of the surface-modified CeO_2 particles changes from positive to negative with an increment in the medium pH while the surface charge of the unmodified CeO_2 particle does not change with varying pH. Long-term dispersion stability test (up to 100 days) shows that the oleic acid-modified nanoparticle with a concentration of 0.3 M retains most stable dispersion in ethylene glycol. The unmodified and decanoic acid-modified nanoparticles with a concentration of 0.03 M precipitate within 7–15 days. In contrast, initial short-term stability evolution reveals different stability behavior compared to the long-term stability. The unmodified and the decanoic acid-modified nanoparticles with a concentration of 0.03 M were less attractive than the oleic acid-modified nanoparticle with 0.3 M. The experimental short-term stability data is in good agreement with the computational results of energy profiles for the CeO_2 nanoparticle suspension.

1. Introduction

Recently, new types of high performance heat transfer fluids have received considerable attention in a variety of areas including microelectronics, chemical plants, transportation, nuclear power station, and HVAC (heating, ventilating, and air conditioning). The thermal conductivity of the heating or cooling fluids plays a vital role in the development of energy-efficient heat transfer equipments. Conventional heat transfer fluids such as water, ethylene glycol, and transformer oil retains poor heat transfer properties [1]. In 1995, Choi introduced a new class of heat transfer fluids, called nanofluids, that can transfer heat more efficiently than the conventional fluids [2]. Nanofluids, in which metal nanoparticles, metal oxide nanoparticles or carbon nanotubes are dispersed in the conventional heat transfer media, can enhance both the thermal conductivity and the heat convection of the base fluids up to two times [3]. Despite the high potential of the nanofluids, agglomeration and rapid settling of the nanoparticles in the base fluids, due to strong interparticle interactions, have been a major obstacle to successful application of the nanofluids [4]. This often causes problems such as severe clogging in micro-channels, corrosion on the pipe's wall, and decrease in the thermal performance of the nanofluids. Therefore, dispersion stability of the nanoparticles in the base fluids has become a primary issue in the research of the nanofluids [5–8].

Surface chemical modification of nanoparticles with appropriate organic ligands is one of the promising methods to attain well-dispersed nanoparticles in liquid media [9,10]. Typically, pre-synthesized nanoparticles were dispersed in a medium and the surface chemical groups of the nanoparticles reacted with the organic ligands. Recently, one-pot synthesis of surface-modified metal oxide nanoparticles in supercritical water (scH_2O) has received much attention due to high diffusivity of reactants in supercritical fluid condition, fast reaction rate, miscibility of organic ligands in scH_2O condition (T_c = 374 °C and P_c = 22.1 MPa), and high reactivity condition. This leads to produce surface-modified nanoparticles in a high rate [11–13]. The hydroxyl groups present on the surface of metal oxide nanoparticles can be replaced with the organic ligands that are miscible in scH_2O condition. Various types of surface-modified nanoparticles including CeO_2, ZnO, AlOOH, Fe_2O_3, $CoAl_2O_4$ and TiO_2 were synthesized in scH_2O using a batch reactor [11,14–17]. More recently, we showed that

* Co-corresponding author. Tel.: +82 2 958 5363; fax: +82 2 958 5205.
** Corresponding author. Tel.: +82 2 958 5874; fax: +82 2 958 5205.
E-mail addresses: mschun@kist.re.kr (M.-S. Chun), jaehoonkim@kist.re.kr (J. Kim).

1385-8947/$ – see front matter.
doi:10.1016/j.cej.2010.12.055

surface-modified cerium oxide (CeO_2) and surface-modified zinc oxide (ZnO) nanoparticles can be synthesized continuously in supercritical methanol (scMeOH, T_c = 240 °C and P_c = 8.1 MPa) using decanoic acid or oleic acid as the surface modifier [18–20]. Inhomogeneous reactant feeding and line/filter clogging problems associated with continuous synthesis of surface-modified nanoparticles in scH_2O can be avoided when scMeOH is used as the continuous reaction medium. The decanoic acid-modified or the oleic acid-modified CeO_2 nanoparticles with diameters in the range of 10–50 nm were synthesized. The surface-modified nanoparticles synthesized in scMeOH showed good dispersion stability in ethylene glycol [18].

Herein, dispersion stability of unmodified, decanoic acid-modified, oleic acid-modified CeO_2 nanoparticles dispersed in ethylene glycol is examined in detail by performing zeta potential measurement, contact angle measurement, long-term stability test (100 days) and short-term stability test (few minutes). The unmodified and the surface-modified CeO_2 nanoparticles were synthesized continuously in supercritical methanol. Even though there are a few reports on the synthesis and the stability of CeO_2 nanocolloids in water or in organic solvents [12,21–24], no information on dispersion stability of surface-modified CeO_2 nanoparticles in ethylene glycol has been reported. In this paper, the stability tests of the surface-modified CeO_2 nanoparticles dispersed in ethylene glycol were performed by measuring optical ultraviolet transmittance variations with time. To gain a better insight into the stability of the surface-modified CeO_2 nanoparticles in ethylene glycol, the experimental stability data were compared with theoretical prediction using an extended DLVO (Derjaguin–Landau–Verwey–Overbeek) theory. For the theoretical prediction, long-range and short-range colloidal interactions are taken into account and each interaction contribution to the overall particle–particle interaction energy is estimated.

2. Interaction energy of nanoparticles

To examine the stability of the unmodified and the surface-modified CeO_2 nanoparticles dispersed in ethylene glycol, the extended-DLVO model of interaction is used. In this model, the net interaction is considered as adding the short-range hydrophobic (or hydrophilic) attraction (or repulsion) into the superposition of the long-range electrostatic double-layer (EDL) repulsion and van der Waals attraction [25]. To estimate these interactions, the diffuse double-layer potential of the particles, the Hamaker constant of the particles in aqueous media, and the acid/base components of the surface free energy of the solids need to be determined. The diffuse double-layer potential can be approximated by the zeta potential from electrophoretic measurements, and the other two quantities can be obtained from contact angle measurements.

According to the previous literature [25–27], the three components of dispersion, induced dipole, and polarization are combined into the Liftshitz–van der Waals component γ^{LW}. The acid/base component γ^{AB} consists of the electrostatic and acceptor–donor interactions, hydrogen bonding, and π bonding. The total surface free energy γ of solid or liquid surface tension can be expressed as

$$\gamma = \gamma^{LW} + \gamma^{AB}. \tag{1}$$

The γ^{AB} component conforms to the equation

$$\gamma^{AB} = 2\sqrt{\gamma^+\gamma^-} \tag{2}$$

where γ^+ and γ^- are the nonadditive parts of the surface free energy of solid or liquid surface tension resulting from electron–acceptor and electron–donor interactions, respectively.

Then, Eq. (1) yields total surface free energy of the solid and the liquid, given as

$$\gamma_S = \gamma_S^{LW} + 2\sqrt{\gamma_S^+\gamma_S^-} \tag{3}$$

$$\gamma_L = \gamma_L^{LW} + 2\sqrt{\gamma_L^+\gamma_L^-} \tag{4}$$

where subscripts S and L denote solid and liquid surfaces, respectively. Using Young's equation, the following relationship can be derived:

$$\gamma_L(1+\cos\theta) = 2\left(\sqrt{\gamma_S^{LW}\gamma_L^{LW}} + \sqrt{\gamma_S^+\gamma_L^-} + \sqrt{\gamma_S^-\gamma_L^+}\right) \tag{5}$$

where θ is the contact angle of the liquid on the solid. By measuring θ for three liquids of known γ_L components, three equations along Eq. (5) are solved in the unknowns γ_S^{LW}, γ_S^+, and γ_S^-.

In this study, the most important potential energies are the electrostatic repulsion E^{EL}, the van der Waals attraction E^{LW}, and the hydrophobic/hydrophilic interaction relating to the acid/base contribution E^{AB}, although the colloidal interactions originate from various forces. Hence, the total interaction can be estimated as follows:

$$E^{TOT}(s) = E^{EL} + E^{LW} + E^{AB} \tag{6}$$

where s means the surface-to-surface distance (i.e., $s = r - 2a$, with r being the center-to-center distance between the particles of radius a). The total interaction force is determined as $F^{TOT}(s) = -dE^{TOT}(s)/ds$.

Many researchers have studied two-particle interactions by using the Poisson–Boltzmann equation [28]. One of the well-known approaches is the Derjaguin approximation when both the EDL thickness (or Debye length) and the separation distance are small compared to the curvature of the surfaces. Taking the constant potential boundary condition at the surfaces, the Derjaguin results for electrostatic repulsion are given by

$$E^{EL}(s) = 2\pi\varepsilon a\zeta^2 \ln\left(1+e^{-\kappa s}\right), \tag{7a}$$

$$F^{EL}(s) = \frac{2\pi\varepsilon\kappa a\zeta^2}{(1+e^{-\kappa s})}e^{-\kappa s}. \tag{7b}$$

Here, ε is the dielectric constant given as a product of the dielectric permittivity of a vacuum ε_o (= 8.854×10^{-12} $C^2/J\,m$) and the relative permittivity ε_r for the dispersion medium and ζ is the electrokinetic zeta potential used as estimation of the diffuse layer potential at the slip plane (or shear surface). The parameter κs corresponds to the surface separation normalized by the EDL thickness κ^{-1} (cf., $\kappa^{-1} = \sqrt{\varepsilon kT/2N_A c_b \Lambda_i^2 e^2}$, where c_b (mM) is the electrolyte ionic concentration in the bulk medium at the electroneutral state, Λ_i the valence of type i ions, e the elementary charge, kT the Boltzmann thermal energy at room temperature), and N_A the Avogadro's number.

Based on a pairwise summation method, the van der Waals attraction between two particles of radius a is quantified by

$$E^{LW}(s) = -\frac{A}{6}\left[\frac{2a^2}{s(4a+s)} + \frac{2a^2}{(2a+s)^2} + \ln\frac{s(4a+s)}{(2a+s)^2}\right], \tag{8a}$$

$$F^{LW}(s) = -\frac{A}{6}\left[\frac{4a^2(2a+s)}{(4as+s^2)^2} + \frac{4a^2}{(2a+s)} - \frac{(4a+2s)(2a+s)-(8as+2s^2)}{s(4a+s)(2a+s)}\right]. \tag{8b}$$

Note that Hamaker constant A can be obtained from the Liftshitz–van der Waals components of the surface free energy of solid and liquid surface tension (i.e., γ_S^{LW} and γ_L^{LW}) as follows:

$$A = 24\pi s_o^2\left(\sqrt{\gamma_S^{LW}} - \sqrt{\gamma_L^{LW}}\right)^2 \tag{9}$$

where s_o can properly be assumed as 1.58 ± 0.08 Å, which are obtained from the literature [25,28].

The last term in Eq. (1) is related to the acid/base contribution to the solid/liquid interfacial free energy, which in turn can be expressed in terms of the electron–acceptor and electron–donor components of the surface free energy of solid and liquid surface tension (i.e., γ_S^+ and γ_S^-, γ_L^+ and γ_L^-) [29]. To represent that contribution, we employ the followings based on the rate of decay with distances,

$$E^{AB}(s) = \Xi_{AB} \exp\left[\frac{s_o - s}{\lambda}\right], \quad (10a)$$

$$F^{AB}(s) = \left(\frac{\Xi_{AB}}{\lambda}\right) \exp\left[\frac{s_o - s}{\lambda}\right] \quad (10b)$$

where

$$\Xi_{AB} = -4\pi a\lambda\left(\sqrt{\gamma_S^+\gamma_S^-} + \sqrt{\gamma_L^+\gamma_L^-} - \sqrt{\gamma_S^+\gamma_L^-} - \sqrt{\gamma_S^-\gamma_L^+}\right). \quad (11)$$

Here, the correlation length of the molecules of the liquid medium λ is taken as 1.0 nm, because it has a reliable value up to ca. 1 nm in the hydrophilic repulsive mode such as ethylene glycol [25,29]. In many cases of hydrophobic attraction, λ may be much larger (e.g., order of 10 nm or more) .

3. Experimental

3.1. Materials

Cerium (III) nitrates hexahydrate ($Ce(NO_3)_3{\cdot}6H_2O$, purity of 99.99%, Kanto Chemicals, Inc.), methanol (HPLC grade, J. T. Baker, Inc.), oleic acid ($CH_3(CH_2)_7CH{=}CH(CH_2)_7COOH$, purity of 99.9%, Daejung Chemicals and Metals, Co.), decanoic acid ($CH_3(CH_2)_8COOH$, purity of 98%, Sigma Aldrich), ethylene glycol (purity of >99%, Yakuri Pure Chemical), diiodomethane (CH_2I_2, purity of 99%, Sigma Aldrich) were used as received. Distilled and deionized (DDI) water was prepared using a Milli-Q, ultrapure water purification system with a 0.22 μm filter (MA, USA).

3.2. Nanoparticle synthesis

The nanoparticle synthesis was carried out using a custom-built continuous flow type reactor as described in the previous work [18]. Only a brief description is given here. All of the CeO_2 nanoparticles synthesized continuously in supercritical water (scH_2O) or in supercritical methanol (scMeOH) at 300 bar and 400 °C. The $Ce(NO_3)_3$ concentration in water or in methanol was 0.05 M. The water or methanol flow rate was fixed to 6 ml/min and the $Ce(NO3)_3$ solution flow rate was fixed to 2 ml/min. The surface-modified CeO_2 with 0.03 M decanoic acid and with 0.3 M oleic acid were synthesized in supercritical methanol. Hereafter, the unmodified CeO_2 particle synthesized in supercritical water is designated as scH_2O + 0, the unmodified CeO_2 particle synthesized in supercritical methanol is designated as scMeOH + 0, the surface-modified CeO_2 with 0.03 M decanoic acid is designated as designated as scMeOH + lDA, and the surface-modified CeO_2 with 0.3 M oleic acid is designated as scMeOH + hOA. As we discussed in the previous paper, the oleic acid-modified CeO_2 nanoparticle and the decanoic acid-modified CeO_2 nanoparticle synthesized at a high concentration of 0.3 M showed very similar dispersion stability in ethylene glycol [18]. In addition, the oleic acid-modified CeO_2 nanoparticle and the decanoic acid-modified CeO_2 nanoparticle synthesized at a low concentration of 0.03 M also showed similar dispersion stability in ethylene glycol. Thus the chain length of the modifiers may play a minor role in the dispersibility of the nanoparticles in ethylene glycol. In this study, the scMeOH + hOA sample was chosen as the representative for the nanoparticle with stable dispersability in ethylene glycol and the scMeOH + lDA was chosen as the representative for the nanoparticle with unstable dispersability in ethylene glycol.

3.3. Analytical methods

Zeta potential of the CeO_2 nanoparticles was measured using an ELS-8000 instrument (Photal Otsuka, Co., Osaka, Japan). For measurement of zeta potential, 0.01 wt% of the CeO_2 nanoparticles was dispersed in ethylene glycol and pH values were adjusted with HCl and NaOH solution using a precise pH meter (Orion 370 PerpHecT Ion Selective Benchtop Meter, Thermo Fisher Scientific Inc., MA, USA). To obtain the consistent electrostatic condition, total ionic strength of 0.4 mM KCl electrolyte was added in the dispersed medium. Contact angle measurements were performed using a CAM 100 contact angle goniometer (KSV Instrument Ltd., Finland) equipped with a CCD camera. The contact angles were measured by slowly injecting 8 μL of the probe liquid. The contact angles reported in this paper represent average values over four measurements performed on each sample. The test liquids were water ($\gamma_L^{LW} = 21.8$, $\gamma_L^{AB} = 51$ ($\gamma_L^+ = \gamma_L^- = 25.5$), $\gamma^L = 72.8$ mJ/m^2), ethylene glycol ($\gamma_L^{LW} = 29.0$, $\gamma_L^{AB} = 18.1$ ($\gamma_L^+ = 1.92$, $\gamma_L^- = 47$), $\gamma_L = 48$ mJ/m^2), and diiodomethane ($\gamma_L^{LW} = 50.8$, $\gamma_L^{AB} = 0$ ($\gamma_L^+ = \gamma_L^- = 0$), $\gamma_L = 50.8$ mJ/m^2) [25,30].

4. Results and discussion

The particle size and degree of surface modification determined using particle size analysis and thermogravimetric analysis [18], and surface free energy of the unmodified and the surface-modified CeO_2 nanoparticles determined by measuring the contact angles of water, ethylene glycol and diodomethane are listed in Table 1. When the high concentration of oleic acid was used, smaller size particles resulted due to inhibition of particle growth by covering the surface of growing particles with the surface-modifiers. By using the thermal gravimetric analysis data and an assumption that the surface modifier is attached on the surface of the primary CeO_2 nanoparticles [31], it was estimated that ~20% of scMeOH + lDA surface and ~19% of the scMeOH + hOA surface were covered by the surface modifiers. The unmodified CeO_2 nanoparticles synthesized in scH_2O or in scMeOH had a low water contact angle of 11.1°, indicating the surface of the particles was hydrophilic. In fact, the surface of the unmodified particles was covered with –OH groups, as determined by Fourier transform infrared (FT-IR) measurement [18,19]. Higher water contact angles were observed in the case of the surface-modified CeO_2 nanoparticles. The water contact angles of the scMeOH + lDA sample increased significantly to 67.7°. Further increase in the water contact angle up to 146.7° was observed when the water contact angle was measured on the surface of scMeOH + hOA. This suggests that the surface of the particles changed from hydrophilic to hydrophobic by covering the surface of the nanoparticles with decanoic acid or oleic acid.

As listed in Table 1, the degree of surface modification of scMeOH + lDA and scMeOH + hOA is similar. Thus the higher water contact angle on scMeOH + hOA than that on scMeOH + lDA is because longer chain length of oleic acid. The contact angles of ethylene glycol and diiodomethane of the surface-modified nanoparticles were also higher than those of the unmodified nanoparticles. Utilizing the values of γ_L^{LW}, γ_L and the contact angle data of the test liquids on the nanoparticles, each component of the solid surface free energy, γ_S^{LW}, γ_S^+, γ_S^-, and γ_S^{AB}, was calculated from Eqs. (1)–(5) and the results are listed in Table 1. It can be seen that γ_S^{LW} is the major contribution to the total surface free energy of the scH_2O + 0, scMeOH + 0 and scMeOH + lDA samples. In case of scMeOH + hOA, the contribution of γ_S^{LW} and γ_S^{AB} to the total surface free energy is very similar. The Hamaker constants of the unmodified and the surface-modified nanoparticles synthesized at the different conditions were then estimated using Eq. (9).

Table 1
Particle size, degree of surface modification, contact angle, each components of solid surface free energy, and parameters of acid/base component for the unmodified and the surface-modified CeO_2 nanoparticles.

Synthetic method	Particle size (nm)	Degree of surface modification (%)	Test liquids	Contact angle (degree)	γ_S^{LW} (mJ/m^2)	γ_S^+ (mJ/m^2)	γ_S^- (mJ/m^2)	γ_S^{AB} (mJ/m^2)
scH_2O+0	91	–	H_2O	11.1 ± 1.6	49.84	0.1225	65.61	0.05
			EG	17.7 ± 0.1				
			CH_2I_2	11.7 ± 1.2				
scMeOH + 0	33	–	H_2O	11.1 ± 0.1	49.5	0.21	67.73	7.54
			EG	22.6 ± 1.8				
			CH_2I_2	13.2 ± 1.9				
scMeOH + lDA	42	20	H_2O	67.7 ± 0.5	49.48	0.26	8.58	3.01
			EG	26.7 ± 1.1				
			CH_2I_2	13.3 ± 2.9				
scMeOH + hOA	12	19	H_2O	146.7 ± 2.4	48.72	3.7	51.7	58.53
			EG	46.2 ± 2.5				
			CH_2I_2	16.7 ± 3.7				

Dispersion stability of particles in a liquid medium is closely related to electrokinetic properties of the dispersed particles. Higher value of surface charge density is beneficial to obtain well-dispersed nanoparticles due to generation of strong repulsive forces between neighboring particles. In general, the surface charge density of a sphere σ_s can be expressed by the electric surface potential Ψ_s as $\sigma_s = \Psi_s(\kappa a + 1)$, where both σ_s and Ψ_s are dimensionless quantities. The charge property of surface is characterized by the electrokinetic zeta potential measurement, but strictly speaking, ζ does not give direct information about the electric surface potential itself. Nonetheless, the experimentally determined ζ values are customarily equivalent to the electric surface potentials [28]. Thus, it is necessary to investigate the electrokinetic behavior using the zeta potential measurements to understand the dispersion behavior of the unmodified and the surface-modified CeO_2 nanoparticles in ethylene glycol.

Fig. 1 shows the zeta potentials of the unmodified and the surface-modified CeO_2 nanoparticles in ethylene glycol at various pH values. The unmodified and the surface-modified CeO_2 nanoparticles synthesized in scMeOH showed similar electrokinetic behavior. When the medium pH increased, the surface charge of the CeO_2 nanoparticles synthesized in scMeOH changed from positive to negative values, where the isoelectric points (IEPs) existed at pH 7.5–8. In contrast to such a behavior of indifferent electrolyte, the surface of the CeO_2 nanoparticles synthesized in scH_2O retained negatively charged surface at all pH ranges with an IEP around pH 6.5. Adding more acid causes an increase in the magnitude of negative zeta potential, which results from a possible shift of the slip plane due to the specifically stronger adsorption of nonhydrated co-ions (Cl^-) in the inner Helmholtz layer than that of hydrated counter-ions (H^+) in the outer Helmholtz layer. Note that these two layers are termed as the Stern layer, and the diffuse layer defined beyond the outer Helmholtz plane contains the slip plane. It is evident that the surface of the CeO_2 nanoparticles synthesized in scMeOH and that of the CeO_2 synthesized in scH_2O become oppositely charged at pH less than 7.5. At pH higher than 8, the surface of the CeO_2 synthesized in scH_2O is considered to be more strongly charged as being due to its higher magnitude of negative zeta potential than those of the CeO_2 particles synthesized in scMeOH.

Fig. 2 shows the long-term (100 days) stability behavior of the unmodified and the surface-modified CeO_2 nanoparticles dispersed in ethylene glycol by measuring the UV transmittance of the suspension. The nanoparticle concentration in ethylene glycol was 0.01 wt%. Just after dispersion of the scH_2O+0, scMeOH + 0, and scMeOH + lDA samples in ethylene glycol, the percentage transmittance of the medium was less than 10%. This indicates that ~90% of the incident UV light was scattered by the dispersed particles in ethylene glycol and did not pass through the medium. The unmodified CeO_2 nanoparticles synthesized in scH_2O were stable during

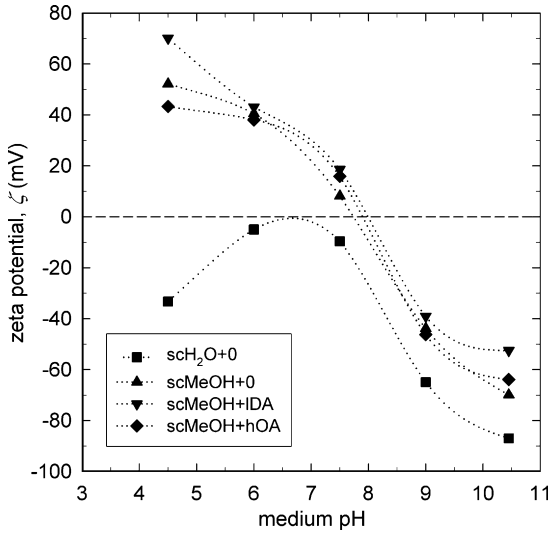

Fig. 1. Zeta potential values of the unmodified and the surface-modified CeO_2 nanoparticles dispersed in ethylene glycol medium at different pH values. The nanoparticle concentration was 0.01 wt%.

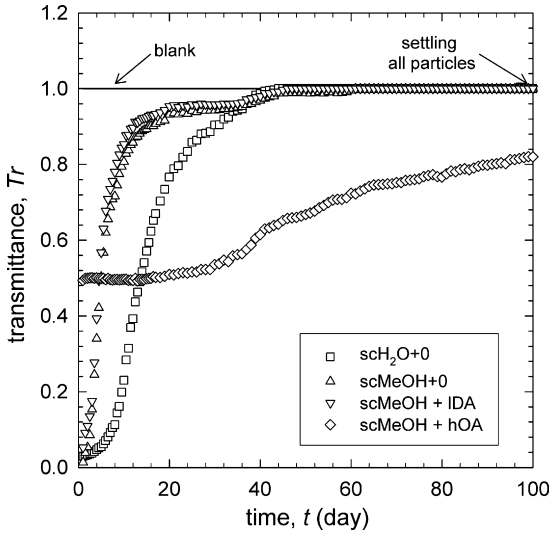

Fig. 2. UV transmittance of the unmodified and the surface-modified CeO_2 nanoparticles dispersed in ethylene glycol medium. The nanoparticle concentration was 0.01 wt%. The measurements were carried out at a wavelength of 400 nm.

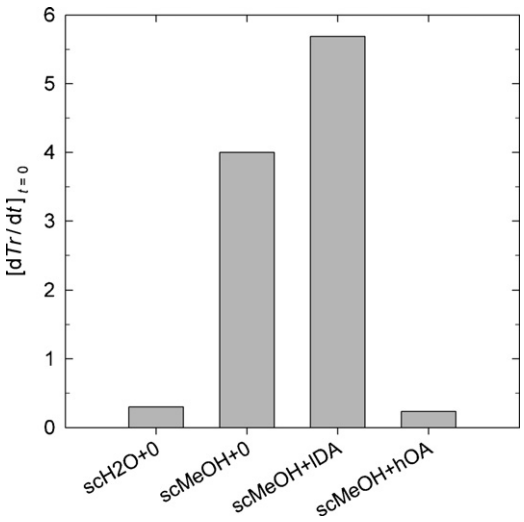

Fig. 3. Initial slopes of transmittance curves provided in Fig. 2 for the unmodified and the surface-modified CeO_2 nanoparticles.

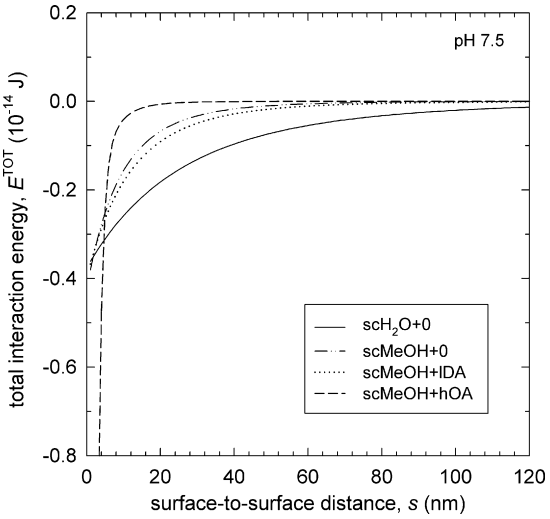

Fig. 4. Total interaction energy profiles for the unmodified and the surface-modified CeO_2 nanoparticles dispersed in ethylene glycol medium at pH 7.5. The nanoparticle concentration was 0.01 wt%.

the first 7 days, and then the particle sedimentation was slowly preceded for the last 40 days. After 40 days, the particles synthesized in scH_2O completely precipitated. The transmittance of the scMeOH + 0 and the scMeOH + lDA samples increased rapidly during the first 3 days and appeared to reach an asymptotic value of ~95% after 14 days. Further transmittance measurement revealed the slower particle settling for the last 40 days. Significantly better long-term stability was observed in the scMeOH + hOA sample. Note that only a slight increase in the transmittance from 49% to 54% was observed during the first 30 days, almost entirely maintaining the slower sedimentation of the particles. It is not clear what is causing an increment around 40 days for the unmodified and the surface-modified nanoparticles that is shown in Fig. 2. The reason may be experimental errors because all the particles showed similar behavior. For practical application of nanofluids, higher concentration of nanoparticles in the range of 0.1–1.0 wt% were typically dispersed in a medium. As shown in Supplementary Material, dispersion stability of the scMeOH + hOA in ethylene glycol at higher concentration (0.1 and 1.0 wt%) was examined for three weeks. The UV transmittance increased only marginally from 0 to 0.1% when the nanoparticles were dispersed in ethylene glycol at concentrations of 0.1 and 1.0 wt% (see Fig. S1). However, it can be seen that some portion of the nanoparticles were still dispersed in ethylene glycol while other portion of the nanoparticles precipitated at the bottom of the vial (see Fig. S2). This indicates that the rate of agglomeration increases with increasing particle concentration.

It is noted that the experimentally obtained transmittance values have meaning only at the initial stages of particle aggregation to compare the experimental results with those from the theoretical calculation. Fig. 3 presents the initial slopes of transmittance curves obtained from short-term stability test at every 40 s intervals for 40 min. The transmittance changes occurred by coupled mechanism including formation of doublets from individual particles and gravitational sedimentation of the particles. The initial slopes of the scH_2O + 0 and the scMeOH + hOA samples are an order of magnitude lower compared to the scMeOH + 0 and scMeOH + lDA samples. The lower values of the slope indicate that the turbidity of the suspension increased at the initial stage of aggregation due to stronger attractive energy between the CeO_2 nanoparticles. In spite of the inevitable presence of the gravitational sedimentation, the net effect would be a slower rate of increase in transmittance. For higher slope estimated in cases of the scMeOH + 0 and the scMeOH + lDA samples, the particle aggregation should also be rapid, and the transmittance increase owing to the gravitational settling is relatively faster than its decrease by the particle aggregation caused by weaker attraction between particles.

The behavior of the initial time variation of transmittance can be related to the computational results of the energy profile. The interaction energy profiles of the unmodified and the surface-modified CeO_2 nanoparticles were calculated using the extended-DLVO model. This model accounts for the effects of the particles size, condition of dispersion medium, and the particle surface properties including the zeta potential and contact angle. Considering the relative permittivity of ethylene glycol at room temperature (i.e., $\varepsilon_r = 40$), the EDL thickness, κ^{-1}, at the around surface of the particles was estimated to be 10.7 nm for the condition of total ionic strength of medium. As shown in Fig. 4, the total interactions were found to be all attractive in the whole range of separation distance between the CeO_2 nanoparticles. This indicates that the particles aggregate at the early stage of dispersion. Although particles were charged with finite values of zeta potential, repulsive interaction resulting from the high screening effect was not observed in Fig. 4. It can be seen that the interaction between the unmodified CeO_2 particles synthesized in scH_2O were more attractive for the entire range of particle separations compared to the scMeOH + 0 and the scMeOH + lDA samples. The profile of the scMeOH + hOA sample was identified as less attractive in the most of modest particle separations, whereas it became dramatically attractive for closer particle separation less than 5 nm. The smaller particles are highly probable to be undertaken the interaction at closer separation.

The attractive forces between the nanoparticles can be attributed to both the van der Waals contribution and the acid/base contribution (cf., hydrophobic attractions), which are directly related to the surface free energy terms. Fig. 5 presents the energy profiles consisting of electrostatic and van der Waals interaction energy. By comparing with Fig. 4, it can be seen that van der Waals interaction is a major contribution to the attraction, except the scMeOH + hOA case. In the extremely short-range of scMeOH + hOA case, the acid/base contribution plays a distinct role. Thus based on the interaction energy analysis, the scMeOH + hOA sample showed the strongest interparticle attraction. However, scMeOH + hOA exhibited the most stable dispersion in ethylene glycol in the long-term test because the long-term stability is determined by hydrodynamic effects.

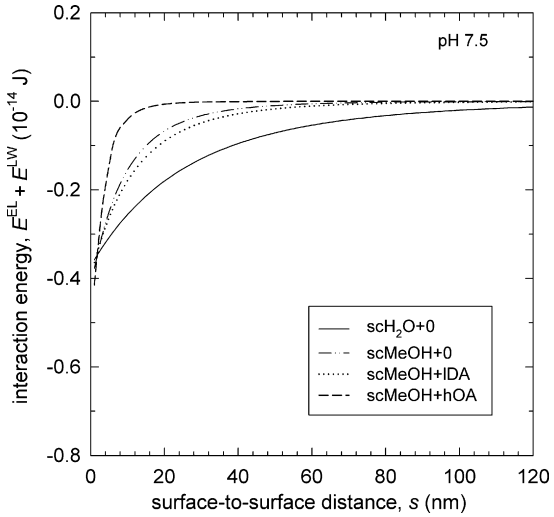

Fig. 5. Electrostatic and van der Waals interaction energy profiles for the unmodified and the surface-modified CeO_2 nanoparticles dispersed in ethylene glycol medium at pH 7.5. The nanoparticle concentration was 0.01 wt%.

5. Conclusions

In order to attain well-dispersed nanoparticles, the surface-modified CeO_2 nanoparticles were synthesized in scMeOH, then the stability of their suspension dispersed in ethylene glycol was studied. In view of the long-term evolution, the surface-modified CeO_2 particles synthesized in scMeOH at the high concentration of surface modifier (scMeOH + hOA) kept the stable dispersion for the 100 days. In contrast, the unmodified CeO_2 particles synthesized in scH_2O or in scMeOH, and the surface-modified CeO_2 particles in scMeOH at the low concentration of surface modifier (scMeOH + lDA) precipitated within 7–15 days. However, the initial short-term evolution revealed different stability behaviors compared to the long-term stability. The scMeOH + 0 and scMeOH + lDA samples were less attractive than the scH_2O + 0 and the scMeOH + hOA samples. In the computational results of energy profiles for each CeO_2 nanoparticle suspension taken into account the extended DLVO theory, the attractive interaction played a major contribution in the total energy, due to the thin EDL thickness around the particles dispersed in ethylene glycol. The extended DLVO theory is applicable to verify the experimental results with reasonable explanation for the behavior of particle dispersion relevant to initial short-term evolution combined with aggregation and sedimentation.

Acknowledgements

This research was supported by Nano R&D program through the National Research Foundation of Korea funded by the Ministry of Education, Science and Technology (2010-0019131). Additional support by the National Research Foundation of Korea Grant funded by the Korean Government (MEST) (NRF-2009-C1A AA001-2009-0092935) was appreciated

Appendix A. Supplementary data

Supplementary data associated with this article can be found, in the online version, at doi:10.1016/j.cej.2010.12.055.

References

[1] S.K. Das, S.U.S. Choi, H.E. Patel, Heat transfer in nanofluids—a review, Heat Transfer Eng. 27 (2006) 3–19.
[2] S.U.S. Choi, Enhancing thermal conductivity of fluids with nanoparticles, in: D.A. Siginer, H.P. Wang (Eds.), Developments and Applications of Non-Newtonian Flows, Vol. FED-Vol. 231/MD-Vol. 66, ASME, New York, 1995, pp. 99–105.
[3] P. Keblinski, J.A. Eastman, D.G. Cahill, Nanofluids for thermal transport, Mater. Today 8 (2005) 36–44.
[4] W. Yu, D.M. France, J.L. Routbort, S.U.S. Choi, Review and comparison of nanofluid thermal conductivity and heat transfer enhancements, Heat Transfer Eng. 29 (2008) 432–460.
[5] Y. Hwang, J.K. Lee, C.H. Lee, Y.M. Jung, S.I. Cheong, C.G. Lee, B.C. Ku, S.P. Jang, Stability and thermal conductivity characteristics of nanofluids, Thermochim. Acta 455 (2007) 70–74.
[6] Y. Hwang, J.-K. Lee, J.-K. Lee, Y.-M. Jeong, S.-I. Cheong, Y.-C. Ahn, S.H. Kim, Production and dispersion stability of nanoparticles in nanofluids, Powder Technol. 186 (2008) 145–153.
[7] M.E. Meibodi, M. Vafaie-Sefti, A.M. Rashidi, A. Amrollahi, M. Tabasi, H.S. Kalal, The role of different parameters on the stability and thermal conductivity of carbon nanotube/water nanofluids, Int. Commun. Heat Mass Transfer 37 (2010) 319–323.
[8] D. Zhu, X. Li, N. Wang, X. Wang, J. Gao, H. Li, Dispersion behavior and thermal conductivity characteristics of Al_2O_3·H_2O nanofluids, Curr. Appl. Phys. 9 (2009) 131–139.
[9] D. Horn, J. Rieger, Organic nanoparticles in the aqueous phase—theory, experiment, and use, Angew. Chem. Int. Ed. 40 (2001) 4331–4361.
[10] H. Bonnemann, G. Braun, W. Brijoux, R. Brinkmann, A.S. Tilling, K. Seevogel, K. Siepen, Nanoscale colloidal metals and alloys stabilized by solvents and surfactants—preparation and use as catalyst precursors, J. Organomet. Chem. 520 (1996) 143–162.
[11] D. Rangappa, T. Naka, A. Kondo, M. Ishii, T. Kobayashi, T. Adschiri, Transparent $CoAl_2O_4$ hybrid nano pigment by organic ligand-assisted supercritical water, J. Am. Chem. Soc. 129 (2007) 11061–11066.
[12] J. Zhang, S. Ohara, M. Umetsu, T. Naka, Y. Hatakeyama, T. Adschiri, Colloidal ceria nanocrystals: a tailor-made crystal morphology in supercritical water, Adv. Mater. 19 (2007) 203–206.
[13] T. Mousavand, S. Takami, M. Umetsu, S. Ohara, T. Adschiri, Supercritical hydrothermal synthesis of organic–inorganic hybrid nanoparticles, J. Mater. Sci. 41 (2006) 1445–1448.
[14] T. Adschiri, Supercritical hydrothermal synthesis of organic–inorganic hybrid nanoparticles, Chem. Lett. 36 (2007) 1188–1193.
[15] T. Mousavand, S. Ohara, M. Umetsu, J. Zhang, S. Takami, T. Naka, T. Adschiri, Hydrothermal synthesis and in situ surface modification of boehmite nanoparticles in supercritical water, J. Supercrit. Fluids 40 (2007) 397–401.
[16] T. Mousavand, J. Zhang, S. Ohara, M. Umetsu, T. Naka, T. Adschiri, Organic-ligand-assisted supercritical hydrothermal synthesis of titanium oxide nanocrystals leading to perfectly dispersed titanium oxide nanoparticle in organic phase, J. Nanopart. Res. 9 (2007) 1067–1071.
[17] S. Takami, T. Sato, T. Mousavand, S. Ohara, M. Umetsu, T. Adschiri, Hydrothermal synthesis of surface-modified iron oxide nanoparticles, Mater. Lett. 61 (2007) 4769–4772.
[18] B. Veriansyah, H. Park, J.-D. Kim, B.K. Min, Y.H. Shin, Y.-W. Lee, J. Kim, Characterization of surface-modified ceria oxide nanoparticles synthesized continuously in supercritical methanol, J. Supercrit. Fluids 50 (2009) 283–291.
[19] J. Kim, Y.-S. Park, B. Veriansyah, J.-D. Kim, Y.-W. Lee, Continuous synthesis of surface-modified metal oxide nanoparticles using supercritical methanol for highly stabilized nanofluids, Chem. Mater. 20 (2008) 6301–6303.
[20] B. Veriansyah, J.-D. Kim, B.K. Min, Y.H. Shin, Y.-W. Lee, J. Kim, Continuous synthesis of surface-modified zinc oxide nanoparticles in supercritical methanol, J. Supercrit. Fluids 52 (2010) 76–83.
[21] M. Nabavi, O. Spalla, B. Cabane, Surface chemistry of nanometric ceria particles in aqueous dispersions, J. Colloid Interface Sci. 160 (1993) 459–471.
[22] S.-H. Yu, H. Colfen, A. Fischer, High quality CeO_2 nanocrystals stabilized by a double hydrophilic block copolymer, Colloids Surf. A: Physicochem. Eng. Aspects 243 (2004) 49–52.
[23] A. Sehgal, Y. Lalatonne, J.F. Berret, M. Morvan, Precipitation–redispersion of cerium oxide nanoparticles with poly(acrylic acid): toward stable dispersions, Langmuir 21 (2005) 9359–9364.
[24] A. Dietrich, A. Neubrand, Y. Hirata, Filtration behavior of nanoparticulate ceria slurries, J. Am. Ceram. Soc. 85 (2002) 2719–2724.
[25] C.J. van Oss, Interfacial Forces in Aqueous Media, first ed., Marcel Dekker, New York, 1994.
[26] F.M. Fowkes, M.A. Mostafa, Acid–base interactions in polymer adsorption, Ind. Eng. Chem. Prod. Res. Dev. 17 (1978) 3–7.
[27] C.J. van Oss, M.K. Chaudhury, R.J. Good, Monopolar surfaces, Adv. Colloid Interface Sci. 28 (1987) 35–64.
[28] J.N. Israelachvili, Intermolecular and Surface Forces, second ed., Academic Press, New York, 1992.
[29] R.C. Plaza, J. de Vicente, S. Gomez-Lopera, A.V. Delgado, Stability of dispersions of colloidal nickel ferrite spheres, J. Colloid Interface Sci. 242 (2001) 306–313.
[30] B. Janczuk, T. Bialopiotrowicz, A. Zdziennicka, Some remarks on the components of the liquid surface free energy, J. Colloid Interface Sci. 211 (1999) 96–103.
[31] K.R. Gopidas, J.K. Whitesell, M.A. Fox, Synthesis, characterization and catalytic applications of a palladium-nanoparticle-cored dendrimer, Nano Lett. 3 (2003) 1757–1760.